

Time-Reversal-Invariant Z_4 Fractional Josephson Effect

Fan Zhang and C. L. Kane - arXiv:1404.1072

We study the Josephson junction mediated by the quantum spin Hall edge states and show that electron-electron interactions lead to a dissipationless fractional Josephson effect in the presence of time-reversal symmetry. Surprisingly, the periodicity is 8π , corresponding to a Josephson frequency $eV/2\hbar$. We estimate the magnitude of interaction induced many-body level splitting responsible for this effect and argue that it can be measured using tunneling spectroscopy. For strong interactions we show that the Josephson effect is associated with the weak tunneling of charge $e/2$ quasiparticles between the superconductors. Our theory describes a fourfold ground state degeneracy that is similar to that of coupled "fractional" Majorana modes, but is protected by time reversal symmetry.

April 8, 2014

Layout

- 1 8 π Josephson effect
 - Single particle spectrum
 - Many-body spectrum
- 2 Phase dependence of the tunneling spectrum of ABSs
 - Ring geometry
 - Ring geometry
- 3 Tunneling of $e/2$ quasiparticles
 - Formalism
 - Hamiltonian in the degenerate ground state

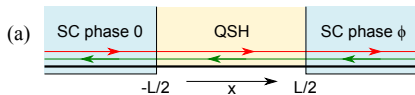


Figure: (a) Schematic of a Josephson junction mediated by the QSH edge states.

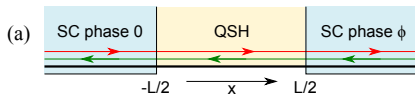


Figure: (a) Schematic of a Josephson junction mediated by the QSH edge states.

- $\mathcal{H}_{BDG} = \tau^z (-i\hbar v_F \sigma^z \partial_x - \mu) + \Delta_1(x) \tau^x + \Delta_2(x) \tau^y,$

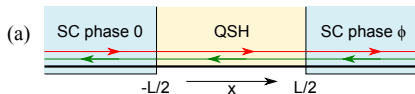


Figure: (a) Schematic of a Josephson junction mediated by the QSH edge states.

- $\mathcal{H}_{BDG} = \tau^z(-i\hbar v_F \sigma^z \partial_x - \mu) + \Delta_1(x)\tau^x + \Delta_2(x)\tau^y$,
- $\vec{\sigma}$ ($\vec{\tau}$) are Pauli matrices in spin (particle-hole) space and $\Delta = \Delta_1 + i\Delta_2$ is the proximity induced pair potential

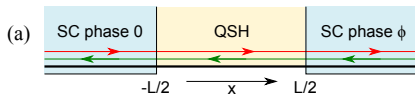


Figure: (a) Schematic of a Josephson junction mediated by the QSH edge states.

- $\mathcal{H}_{BDG} = \tau^z (-i\hbar v_F \sigma^z \partial_x - \mu) + \Delta_1(x) \tau^x + \Delta_2(x) \tau^y$,
- $\vec{\sigma}$ ($\vec{\tau}$) are Pauli matrices in spin (particle-hole) space and $\Delta = \Delta_1 + i\Delta_2$ is the proximity induced pair potential
- $\Delta(x < -L/2) = \Delta_0$, $\Delta(x > L/2) = \Delta_0 e^{i\phi}$, and $\Delta(|x| < L/2) = 0$

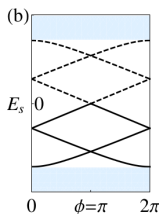


Figure: (b) The single-particle BdG spectrum of the junction as a function of ϕ , with Kramers degeneracies at $\phi = 0$ and π .

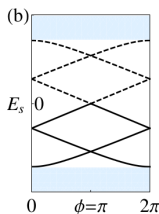


Figure: (b) The single-particle BdG spectrum of the junction as a function of ϕ , with Kramers degeneracies at $\phi = 0$ and π .

- Andreev bound states (ABS) spectrum \rightarrow solving \mathcal{H}_{BdG} , with appropriate boundary conditions

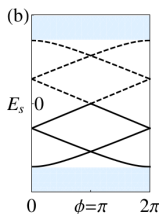


Figure: (b) The single-particle BdG spectrum of the junction as a function of ϕ , with Kramers degeneracies at $\phi = 0$ and π .

- Andreev bound states (ABS) spectrum \rightarrow solving \mathcal{H}_{BdG} , with appropriate boundary conditions
- $L > hv_F/(4\Delta_0) \Rightarrow$ at least one pair of excited bound states

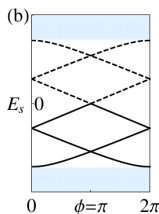


Figure: (b) The single-particle BdG spectrum of the junction as a function of ϕ , with Kramers degeneracies at $\phi = 0$ and π .

$$\bullet \psi_{n,\sigma} = \begin{pmatrix} u_{n,\sigma} \\ v_{n,\sigma} \end{pmatrix} = \mathcal{A}_n(x) \begin{pmatrix} (-1)^n e^{i\sigma \bar{E}_n \bar{\ell}(x)} \\ -i\sigma e^{-i\sigma \bar{E}_n \bar{\ell}(x)} \end{pmatrix},$$

$$\mathcal{A}_n(x) = 1 \sqrt{2L + 2\xi(1 - \bar{E}_n^2)^{-1/2}} e^{i\sigma \bar{\mu} \bar{x} - \sqrt{1 - \bar{E}_n^2} |\bar{x} - \bar{\ell}(x)|}$$

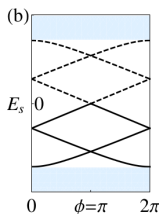


Figure: (b) The single-particle BdG spectrum of the junction as a function of ϕ , with Kramers degeneracies at $\phi = 0$ and π .

- $$\psi_{n,\sigma} = \begin{pmatrix} u_{n,\sigma} \\ v_{n,\sigma} \end{pmatrix} = \mathcal{A}_n(x) \begin{pmatrix} (-1)^n e^{i\sigma \bar{E}_n \bar{\ell}(x)} \\ -i\sigma e^{-i\sigma \bar{E}_n \bar{\ell}(x)} \end{pmatrix},$$

$$\mathcal{A}_n(x) = 1 \sqrt{2L + 2\xi(1 - \bar{E}_n^2)^{-1/2}} e^{i\sigma \bar{\mu} \bar{x} - \sqrt{1 - \bar{E}_n^2} |\bar{x} - \bar{\ell}(x)|}$$

- $\bar{E}_n \equiv E_n/\Delta_0$, $\bar{L} \equiv L/\xi = L\Delta_0/\hbar v_F$, $\bar{\ell}(x) = \text{sgn}(x)\bar{L}/2$ in central region, and x/ξ elsewhere, $\bar{\mu} = \mu/\Delta$, $\bar{x} = x/\xi$

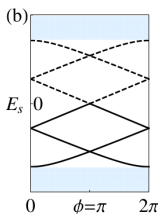


Figure: (b) The single-particle BdG spectrum of the junction as a function of ϕ , with Kramers degeneracies at $\phi = 0$ and π .

$$\bullet \psi_{n,\sigma} = \begin{pmatrix} u_{n,\sigma} \\ v_{n,\sigma} \end{pmatrix} = \mathcal{A}_n(x) \begin{pmatrix} (-1)^n e^{i\sigma \bar{E}_n \bar{\ell}(x)} \\ -i\sigma e^{-i\sigma \bar{E}_n \bar{\ell}(x)} \end{pmatrix},$$

$$\mathcal{A}_n(x) = 1/\sqrt{2L + 2\xi(1 - \bar{E}_n^2)^{-1/2}} e^{i\sigma \bar{\mu} \bar{x} - \sqrt{1 - \bar{E}_n^2} |\bar{x} - \bar{\ell}(x)|}$$

- $\bar{E}_n \equiv E_n/\Delta_0$, $\bar{L} \equiv L/\xi = L\Delta_0/\hbar v_F$, $\bar{\ell}(x) = \text{sgn}(x)\bar{L}/2$ in central region, and x/ξ elsewhere, $\bar{\mu} = \mu/\Delta$, $\bar{x} = x/\xi$
- $E_{-n} = -E_n$ and $\psi_{-n,\sigma} = -i\tau^y \psi_{n,\sigma}$ ($n > 0$)

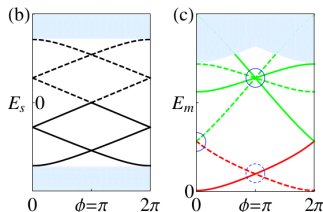


Figure: (c) The spectrum of many-body states corresponding to (b), including a fourfold degeneracy at $\phi = \pi$.

- The lowest state corresponds to the many-body ground state with all positive (negative) energy single-particle states in (b) empty (occupied), whereas higher states are excitations with one or more quasiparticles excited.

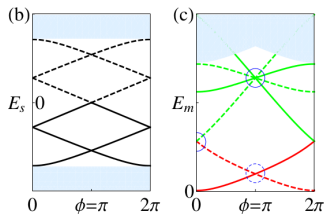


Figure: (c) The spectrum of many-body states corresponding to (b), including a fourfold degeneracy at $\phi = \pi$.

- ABS: $b_{-n,\sigma} = \sigma b_{n,-\sigma}^\dagger$ ($n > 0$) and $b_{0,+} = ib_{0,-}^\dagger$

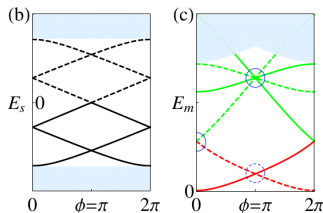


Figure: (c) The spectrum of many-body states corresponding to (b), including a fourfold degeneracy at $\phi = \pi$.

- ABS: $b_{-n,\sigma} = \sigma b_{n,-\sigma}^\dagger$ ($n > 0$) and $b_{0,+} = ib_{0,-}^\dagger$
- $H(\phi) | \Phi_n(\phi) \rangle = \epsilon_n(\phi) | \Phi_n(\phi) \rangle$, $\epsilon_n(\phi) = \sum_m E_m(\phi)(n_m - \frac{1}{2})$

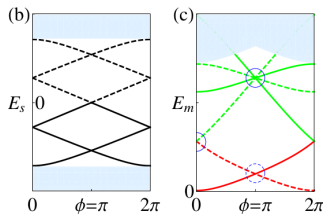


Figure: (c) The spectrum of many-body states corresponding to (b), including a fourfold degeneracy at $\phi = \pi$.

- ABS: $b_{-n,\sigma} = \sigma b_{n,-\sigma}^\dagger$ ($n > 0$) and $b_{0,+} = ib_{0,-}^\dagger$
- $H(\phi) | \Phi_n(\phi) \rangle = \epsilon_n(\phi) | \Phi_n(\phi) \rangle$, $\epsilon_n(\phi) = \sum_m E_m(\phi)(n_m - \frac{1}{2})$
- $| \Phi_n(\phi) \rangle = b_N^{\dagger n_N} \dots b_1^{\dagger n_1} | 0 \rangle$, $n_m = \{0, 1\} \equiv$ occupation probability of m^{th} ABS

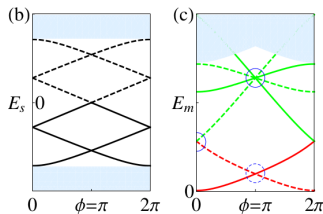


Figure: (c) The spectrum of many-body states corresponding to (b), including a fourfold degeneracy at $\phi = \pi$.

- $\epsilon_n(\phi) = \sum_m E_m(\phi)(n_m - \frac{1}{2}), E_{-n} = -E_n$

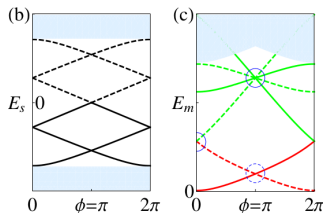


Figure: (c) The spectrum of many-body states corresponding to (b), including a fourfold degeneracy at $\phi = \pi$.

- $\epsilon_n(\phi) = \sum_m E_m(\phi)(n_m - \frac{1}{2})$, $E_{-n} = -E_n$
- Calculate ground state many body energy $\epsilon_0(\phi = 0)$

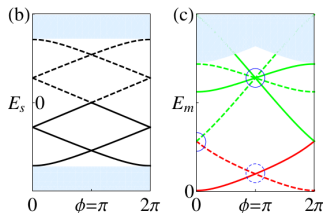


Figure: (c) The spectrum of many-body states corresponding to (b), including a fourfold degeneracy at $\phi = \pi$.

- $\epsilon_n(\phi) = \sum_m E_m(\phi)(n_m - \frac{1}{2})$, $E_{-n} = -E_n$
- Calculate ground state many body energy $\epsilon_0(\phi = 0)$
- Now, ground state many body energy $\epsilon_0(\phi = \pi/2, 3\pi/2)$

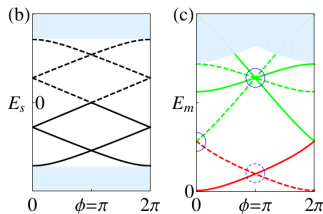


Figure: (c) The spectrum of many-body states corresponding to (b), including a fourfold degeneracy at $\phi = \pi$.

- $\epsilon_n(\phi) = \sum_m E_m(\phi)(n_m - \frac{1}{2})$, $E_{-n} = -E_n$
- Calculate ground state many body energy $\epsilon_0(\phi = 0)$
- Now, ground state many body energy $\epsilon_0(\phi = \pi/2, 3\pi/2)$
- Solid and dashed \equiv different local fermion parity

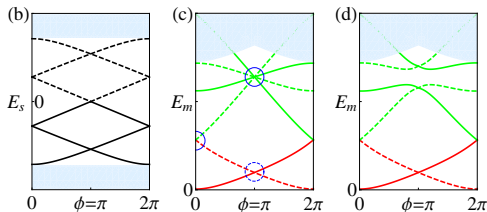


Figure: (d) The fourfold degeneracy is lifted by electron-electron interactions, leading to an 8π periodicity of the four lowest states.

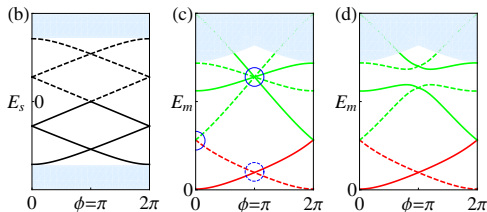


Figure: (d) The fourfold degeneracy is lifted by electron-electron interactions, leading to an 8π periodicity of the four lowest states.

- In the presence of electron-electron interactions it splits into two Kramer doublets, each of which has two many-body states with opposite fermion parity.

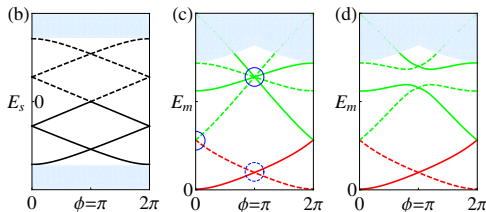


Figure: (d) The fourfold degeneracy is lifted by electron-electron interactions, leading to an 8π periodicity of the four lowest states.

- In the presence of electron-electron interactions it splits into two Kramers doublets, each of which has two many-body states with opposite fermion parity.
- It takes four cycles to return to the original ground state, leading to an 8π periodicity in the current phase relation

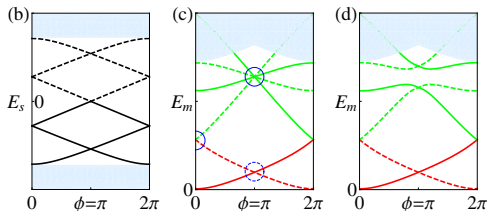


Figure: (d) The fourfold degeneracy is lifted by electron-electron interactions, leading to an 8π periodicity of the four lowest states.

- $\mathcal{H} = \mathcal{H}_0 + \mathcal{H}_I$, $\mathcal{H}_I = \lambda \int_{-L/2}^{L/2} n(x)^2$

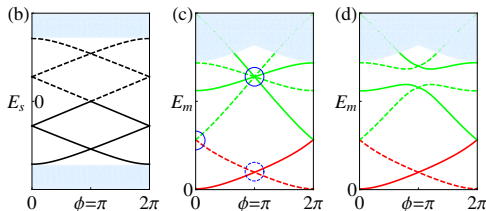


Figure: (d) The fourfold degeneracy is lifted by electron-electron interactions, leading to an 8π periodicity of the four lowest states.

- $\mathcal{H} = \mathcal{H}_0 + \mathcal{H}_I$, $\mathcal{H}_I = \lambda \int_{-L/2}^{L/2} n(x)^2$
- $n(x) = \sum_{\sigma} c_{\sigma}^{\dagger} c_{\sigma}$ is the charge density

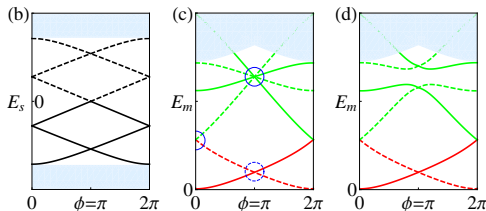


Figure: (d) The fourfold degeneracy is lifted by electron-electron interactions, leading to an 8π periodicity of the four lowest states.

- $\mathcal{H} = \mathcal{H}_0 + \mathcal{H}_I$, $\mathcal{H}_I = \lambda \int_{-L/2}^{L/2} n(x)^2$
- $n(x) = \sum_{\sigma} c_{\sigma}^{\dagger} c_{\sigma}$ is the charge density
- Evaluate matrix elements of \mathcal{H}_I between degenerate many-body states

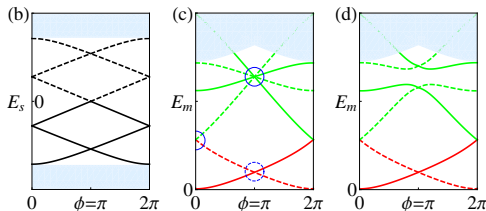


Figure: (d) The fourfold degeneracy is lifted by electron-electron interactions, leading to an 8π periodicity of the four lowest states.

- $\mathcal{H} = \mathcal{H}_0 + \mathcal{H}_I$, $\mathcal{H}_I = \lambda \int_{-L/2}^{L/2} n(x)^2$
- $n(x) = \sum_{\sigma} c_{\sigma}^{\dagger} c_{\sigma}$ is the charge density
- Evaluate matrix elements of \mathcal{H}_I between degenerate many-body states
- $c_{\sigma}(x) = u_{0,\sigma} b_{0,\sigma} + \sum_{n>0} u_{n,\sigma} b_{n,\sigma} - v_{n,\sigma} \sigma b_{n,-\sigma}^{\dagger}$

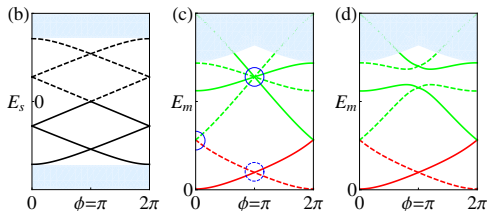


Figure: (d) The fourfold degeneracy is lifted by electron-electron interactions, leading to an 8π periodicity of the four lowest states.

- 4 degenerate many body states are $|\mu, \sigma\rangle = b_{1,\sigma}^\dagger |\mu\rangle_0$

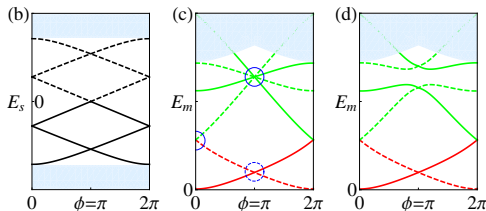


Figure: (d) The fourfold degeneracy is lifted by electron-electron interactions, leading to an 8π periodicity of the four lowest states.

- 4 degenerate many body states are $|\mu, \sigma\rangle = b_{1,\sigma}^\dagger |\mu\rangle_0$
- $|\mu\rangle_0$ is many body ground state $b_{n,\sigma}^\dagger b_{n,\sigma} |\mu\rangle_0 = 0$ ($n > 0$)

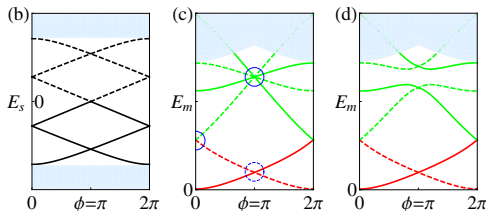


Figure: (d) The fourfold degeneracy is lifted by electron-electron interactions, leading to an 8π periodicity of the four lowest states.

- 4 degenerate many body states are $|\mu, \sigma\rangle = b_{1,\sigma}^\dagger |\mu\rangle_0$
- $|\mu\rangle_0$ is many body ground state $b_{n,\sigma}^\dagger b_{n,\sigma} |\mu\rangle_0 = 0$ ($n > 0$)
- $\mu = (-1)^{b_{0,+}^\dagger b_{0,+}}$ is the fermion parity

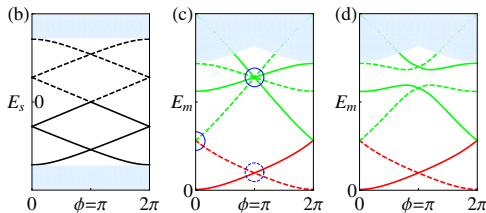


Figure: (d) The fourfold degeneracy is lifted by electron-electron interactions, leading to an 8π periodicity of the four lowest states.

- At $\phi = \pi$, the splitting due to \mathcal{H}_I becomes

$$\delta \sim 2\lambda \int_{-L/2}^{L/2} dx |u_{1,+}^* u_{0,-} - i u_{-1,-} u_{0,+}^*|^2 = \frac{\lambda}{\xi} \left(\frac{1}{\sqrt{1-E_1^2}} + \bar{L} \right)^{-1}$$

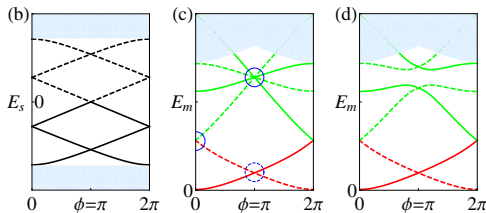


Figure: (d) The fourfold degeneracy is lifted by electron-electron interactions, leading to an 8π periodicity of the four lowest states.

- At $\phi = \pi$, the splitting due to \mathcal{H}_I becomes

$$\delta \sim 2\lambda \int_{-L/2}^{L/2} dx |u_{1,+}^* u_{0,-} - i u_{-1,-} u_{0,+}^*|^2 = \frac{\lambda}{\xi} \left(\frac{1}{\sqrt{1-E_1^2}} + \bar{L} \right)^{-1}$$

- $\bar{L} \sim 2.6$, $\delta \sim 0.23\lambda/\xi$, $\lambda = (e^2/\epsilon) \log(R_s/R)$

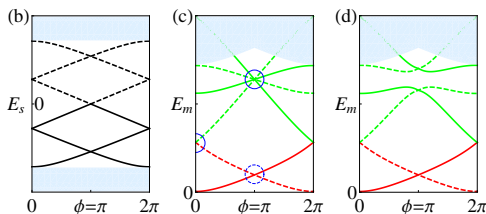


Figure: (d) The fourfold degeneracy is lifted by electron-electron interactions, leading to an 8π periodicity of the four lowest states.

- At $\phi = \pi$, the splitting due to \mathcal{H}_I becomes

$$\delta \sim 2\lambda \int_{-L/2}^{L/2} dx |u_{1,+}^* u_{0,-} - i u_{-1,-} u_{0,+}^*|^2 = \frac{\lambda}{\xi} \left(\frac{1}{\sqrt{1-E_1^2}} + \bar{L} \right)^{-1}$$

- $\bar{L} \sim 2.6$, $\delta \sim 0.23\lambda/\xi$, $\lambda = (e^2/\epsilon) \log(R_s/R)$
- $R, R_s \equiv$ penetration and screening radius of the edge states

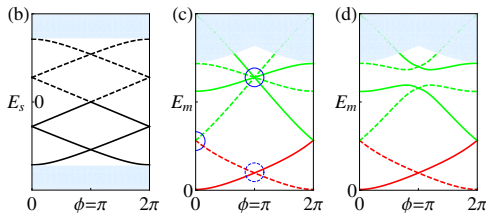


Figure: (d) The fourfold degeneracy is lifted by electron-electron interactions, leading to an 8π periodicity of the four lowest states.

- At $\phi = \pi$, the splitting due to \mathcal{H}_I becomes

$$\delta \sim 2\lambda \int_{-L/2}^{L/2} dx |u_{1,+}^* u_{0,-} - i u_{-1,-} u_{0,+}^*|^2 = \frac{\lambda}{\xi} \left(\frac{1}{\sqrt{1-E_1^2}} + \bar{L} \right)^{-1}$$

- $\bar{L} \sim 2.6$, $\delta \sim 0.23\lambda/\xi$, $\lambda = (e^2/\epsilon) \log(R_s/R)$
- $R, R_s \equiv$ penetration and screening radius of the edge states
- $\epsilon = 20$, $\xi = 100$ nm, and $\log(R_s/R) = 1 \Rightarrow \delta \sim 0.17$ meV

Layout

- 1 8 π Josephson effect
 - Single particle spectrum
 - Many-body spectrum
- 2 Phase dependence of the tunneling spectrum of ABSs
 - Ring geometry
 - Ring geometry
- 3 Tunneling of $e/2$ quasiparticles
 - Formalism
 - Hamiltonian in the degenerate ground state

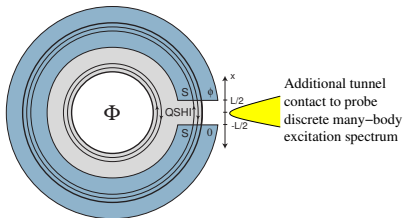


Figure: At low temperatures, weakly coupled tunnel junction probes the local tunneling density of states $dI/dV \propto \rho(E = eV)$

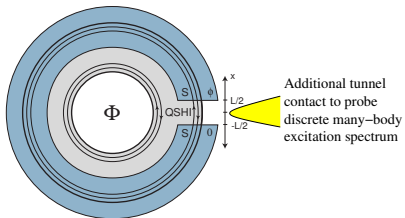


Figure: At low temperatures, weakly coupled tunnel junction probes the local tunneling density of states $dI/dV \propto \rho(E = eV)$

- $$\rho(E) = \sum_{N,\sigma} |\langle N | c_{\sigma}^{\dagger} | 0 \rangle|^2 \delta(E - E_N + E_0)$$

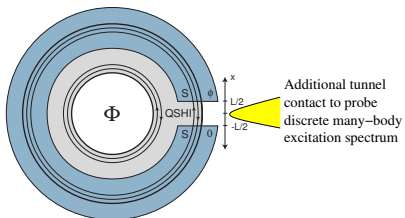


Figure: At low temperatures, weakly coupled tunnel junction probes the local tunneling density of states $dI/dV \propto \rho(E = eV)$

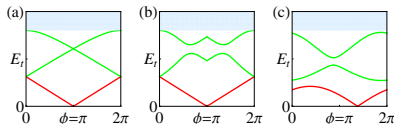
- $\rho(E) = \sum_{N,\sigma} |\langle N | c_{\sigma}^{\dagger} | 0 \rangle|^2 \delta(E - E_N + E_0)$
- c_{σ}^{\dagger} is the creation operator for an electron with spin σ in the junction and $|N\rangle$ are the many-body states

- Selection rule: $|N\rangle$ has opposite parity as compared to $|0\rangle$

- Selection rule: $|N\rangle$ has opposite parity as compared to $|0\rangle$
- dI/dV must consist of peaks at $eV = \epsilon_N - \epsilon_0$

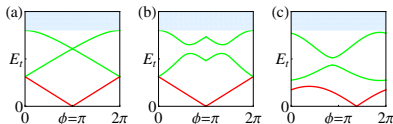


- Selection rule: $|N\rangle$ has opposite parity as compared to $|0\rangle$
- dI/dV must consist of peaks at $eV = \epsilon_N - \epsilon_0$

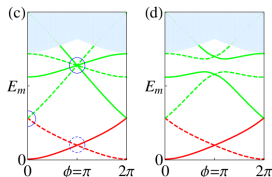


- Phase dependence of the energies of peaks in the tunneling density of states. In the non-interacting case (a) shows a degeneracy at $\phi = \pi$ that is lifted in (b) by interactions. Breaking TRS lifts both degeneracies in (a), as shown in (c).

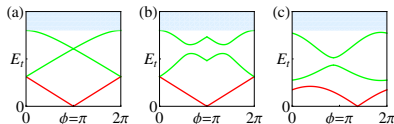
- Selection rule: $|N\rangle$ has opposite parity as compared to $|0\rangle$
- dI/dV must consist of peaks at $eV = \epsilon_N - \epsilon_0$



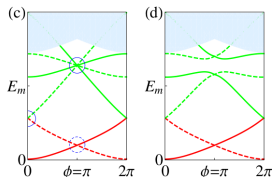
- Phase dependence of the energies of peaks in the tunneling density of states. In the non-interacting case (a) shows a degeneracy at $\phi = \pi$ that is lifted in (b) by interactions. Breaking TRS lifts both degeneracies in (a), as shown in (c).



- Selection rule: $|N\rangle$ has opposite parity as compared to $|0\rangle$
- dI/dV must consist of peaks at $eV = \epsilon_N - \epsilon_0$



- Phase dependence of the energies of peaks in the tunneling density of states. In the non-interacting case (a) shows a degeneracy at $\phi = \pi$ that is lifted in (b) by interactions. Breaking TRS lifts both degeneracies in (a), as shown in (c).

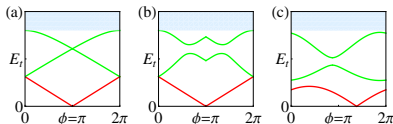


- Singularity lowest peak goes to zero

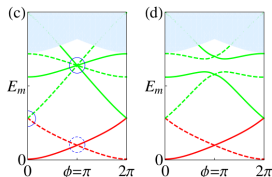


Ring geometry

- Selection rule: $|N\rangle$ has opposite parity as compared to $|0\rangle$
- dI/dV must consist of peaks at $eV = \epsilon_N - \epsilon_0$



- Phase dependence of the energies of peaks in the tunneling density of states. In the non-interacting case (a) shows a degeneracy at $\phi = \pi$ that is lifted in (b) by interactions. Breaking TRS lifts both degeneracies in (a), as shown in (c).

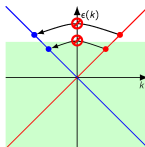


- Singularity lowest peak goes to zero
- TRS breaking shifts this singularity

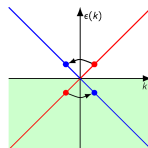
Layout

- 1 8 π Josephson effect
 - Single particle spectrum
 - Many-body spectrum
- 2 Phase dependence of the tunneling spectrum of ABSs
 - Ring geometry
 - Ring geometry
- 3 Tunneling of $e/2$ quasiparticles
 - Formalism
 - Hamiltonian in the degenerate ground state

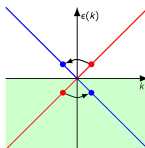
- Pair backscattering term $\propto c_{L\downarrow}^\dagger c_{L\downarrow}^\dagger c_{R\uparrow} c_{R\uparrow}$



- Pair backscattering term $\propto c_{L\downarrow}^\dagger c_{L\downarrow}^\dagger c_{R\uparrow} c_{R\uparrow}$
- Momentum conserving process at $\mu = 0$

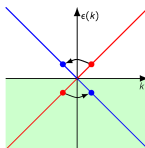


- Pair backscattering term $\propto c_{L\downarrow}^\dagger c_{L\downarrow}^\dagger c_{R\uparrow} c_{R\uparrow}$
- Momentum conserving process at $\mu = 0$
- Bosonization $c_{R\uparrow(L\downarrow)}^\dagger \propto e^{i(\varphi \pm \theta)}$ where
 $[\varphi(x), \theta(x')] = i\pi\Theta(x - x')$



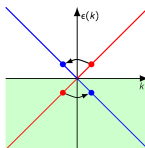
Formalism

- Pair backscattering term $\propto c_{L\downarrow}^\dagger c_{L\downarrow}^\dagger c_{R\uparrow} c_{R\uparrow}$
- Momentum conserving process at $\mu = 0$
- Bosonization $c_{R\uparrow(L\downarrow)}^\dagger \propto e^{i(\varphi \pm \theta)}$ where
 $[\varphi(x), \theta(x')] = i\pi\Theta(x - x')$
- $\mathcal{H} = \mathcal{H}_0 + \mathcal{H}_I + \mathcal{H}_\theta + \mathcal{H}_\varphi$

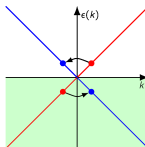


Formalism

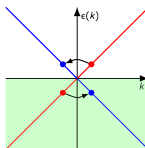
- Pair backscattering term $\propto c_{L\downarrow}^\dagger c_{L\downarrow}^\dagger c_{R\uparrow} c_{R\uparrow}$
- Momentum conserving process at $\mu = 0$
- Bosonization $c_{R\uparrow(L\downarrow)}^\dagger \propto e^{i(\varphi \pm \theta)}$ where
 $[\varphi(x), \theta(x')] = i\pi\Theta(x - x')$
- $\mathcal{H} = \mathcal{H}_0 + \mathcal{H}_I + \mathcal{H}_\theta + \mathcal{H}_\varphi$
- $\mathcal{H}_0 + \mathcal{H}_I = \frac{v_F}{2\pi} [(\partial_x \theta)^2 + (\partial_x \varphi)^2] + \frac{\lambda(x)}{\pi^2} (\partial_x \theta)^2$



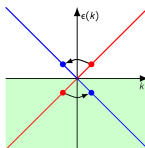
- Pair backscattering term $\propto c_{L\downarrow}^\dagger c_{L\downarrow}^\dagger c_{R\uparrow} c_{R\uparrow}$
- Momentum conserving process at $\mu = 0$
- Bosonization $c_{R\uparrow(L\downarrow)}^\dagger \propto e^{i(\varphi \pm \theta)}$ where
 $[\varphi(x), \theta(x')] = i\pi\Theta(x - x')$
- $\mathcal{H} = \mathcal{H}_0 + \mathcal{H}_I + \mathcal{H}_\theta + \mathcal{H}_\varphi$
- $\mathcal{H}_0 + \mathcal{H}_I = \frac{v_F}{2\pi} [(\partial_x \theta)^2 + (\partial_x \varphi)^2] + \frac{\lambda(x)}{\pi^2} (\partial_x \theta)^2$
- $\mathcal{H}_\varphi = u_0 \left[\Theta(-\frac{L}{2} - x) \cos 2\varphi + \Theta(x - \frac{L}{2}) \cos(2\varphi - \phi) \right]$



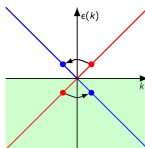
- Pair backscattering term $\propto c_{L\downarrow}^\dagger c_{L\downarrow}^\dagger c_{R\uparrow} c_{R\uparrow}$
- Momentum conserving process at $\mu = 0$
- Bosonization $c_{R\uparrow(L\downarrow)}^\dagger \propto e^{i(\varphi \pm \theta)}$ where
 $[\varphi(x), \theta(x')] = i\pi \Theta(x - x')$
- $\mathcal{H} = \mathcal{H}_0 + \mathcal{H}_I + \mathcal{H}_\theta + \mathcal{H}_\varphi$
- $\mathcal{H}_0 + \mathcal{H}_I = \frac{v_F}{2\pi} [(\partial_x \theta)^2 + (\partial_x \varphi)^2] + \frac{\lambda(x)}{\pi^2} (\partial_x \theta)^2$
- $\mathcal{H}_\varphi = u_0 \left[\Theta(-\frac{L}{2} - x) \cos 2\varphi + \Theta(x - \frac{L}{2}) \cos(2\varphi - \phi) \right]$
- $\mathcal{H}_\theta = v_0 \Theta(\frac{L}{2} - |x|) \cos 4\theta$



- Pair backscattering term $\propto c_{L\downarrow}^\dagger c_{L\downarrow}^\dagger c_{R\uparrow} c_{R\uparrow}$
- Momentum conserving process at $\mu = 0$
- Bosonization $c_{R\uparrow(L\downarrow)}^\dagger \propto e^{i(\varphi \pm \theta)}$ where
 $[\varphi(x), \theta(x')] = i\pi\Theta(x - x')$
- $\mathcal{H} = \mathcal{H}_0 + \mathcal{H}_I + \mathcal{H}_\theta + \mathcal{H}_\varphi$
- $\mathcal{H}_0 + \mathcal{H}_I = \frac{v_F}{2\pi} [(\partial_x \theta)^2 + (\partial_x \varphi)^2] + \frac{\lambda(x)}{\pi^2} (\partial_x \theta)^2$
- $\mathcal{H}_\varphi = u_0 [\Theta(-\frac{L}{2} - x) \cos 2\varphi + \Theta(x - \frac{L}{2}) \cos(2\varphi - \phi)]$
- $\mathcal{H}_\theta = v_0 \Theta(\frac{L}{2} - |x|) \cos 4\theta$
- For large v_0 , θ is pinned in *four* distinct deep wells of the cosine potential

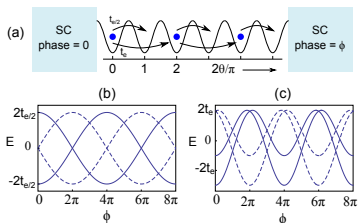


- Pair backscattering term $\propto c_{L\downarrow}^\dagger c_{L\downarrow}^\dagger c_{R\uparrow} c_{R\uparrow}$
- Momentum conserving process at $\mu = 0$
- Bosonization $c_{R\uparrow(L\downarrow)}^\dagger \propto e^{i(\varphi \pm \theta)}$ where $[\varphi(x), \theta(x')] = i\pi\Theta(x - x')$
- $\mathcal{H} = \mathcal{H}_0 + \mathcal{H}_I + \mathcal{H}_\theta + \mathcal{H}_\varphi$
- $\mathcal{H}_0 + \mathcal{H}_I = \frac{v_F}{2\pi} [(\partial_x \theta)^2 + (\partial_x \varphi)^2] + \frac{\lambda(x)}{\pi^2} (\partial_x \theta)^2$
- $\mathcal{H}_\varphi = u_0 \left[\Theta(-\frac{L}{2} - x) \cos 2\varphi + \Theta(x - \frac{L}{2}) \cos(2\varphi - \phi) \right]$
- $\mathcal{H}_\theta = v_0 \Theta(\frac{L}{2} - |x|) \cos 4\theta$
- For large v_0 , θ is pinned in *four* distinct deep wells of the cosine potential
- Quantum tunneling between the 4 minimas (finite v_0 , T) will couple the ground states, lifting their degeneracy with a characteristic pattern



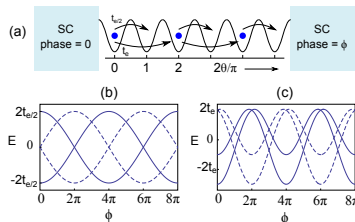


Hamiltonian in the degenerate ground state



- (a) Strong interactions pin the charge between the superconductors and lead to a fourfold ground state degeneracy. Charge $e/2$ or charge e tunneling processes lift the degeneracy, with an 8π periodicity in ϕ , as shown in (b) for $t_e = 0$ and (c) for $t_e = 2t_{e/2}$. Solid and dashed lines correspond to states with opposite fermion parity.

Hamiltonian in the degenerate ground state

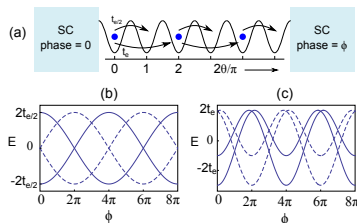


- (a) Strong interactions pin the charge between the superconductors and lead to a fourfold ground state degeneracy. Charge $e/2$ or charge e tunneling processes lift the degeneracy, with an 8π periodicity in ϕ , as shown in (b) for $t_e = 0$ and (c) for $t_e = 2t_{e/2}$. Solid and dashed lines correspond to states with opposite fermion parity.

- $|n\rangle$ denotes the state $\theta = n\pi/2$, (with n defined modulo 4)



Hamiltonian in the degenerate ground state

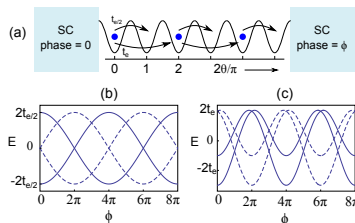


- (a) Strong interactions pin the charge between the superconductors and lead to a fourfold ground state degeneracy. Charge $e/2$ or charge e tunneling processes lift the degeneracy, with an 8π periodicity in ϕ , as shown in (b) for $t_e = 0$ and (c) for $t_e = 2t_{e/2}$. Solid and dashed lines correspond to states with opposite fermion parity.

- $|n\rangle$ denotes the state $\theta = n\pi/2$, (with n defined modulo 4)
- $H = \sum_{n=1}^4 (-t_{e/2} e^{i\frac{\phi}{4}} |n\rangle\langle n+1| - t_e e^{i\frac{\phi}{2}} |n\rangle\langle n+2| + \text{h.c.})$



Hamiltonian in the degenerate ground state

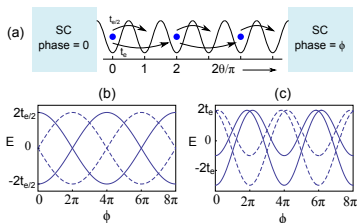


(a) Strong interactions pin the charge between the superconductors and lead to a fourfold ground state degeneracy. Charge $e/2$ or charge e tunneling processes lift the degeneracy, with an 8π periodicity in ϕ , as shown in (b) for $t_e = 0$ and (c) for $t_e = 2t_{e/2}$. Solid and dashed lines correspond to states with opposite fermion parity.

- $|n\rangle$ denotes the state $\theta = n\pi/2$, (with n defined modulo 4)
- $H = \sum_{n=1}^4 (-t_{e/2} e^{i\frac{\phi}{4}} |n\rangle\langle n+1| - t_e e^{i\frac{\phi}{2}} |n\rangle\langle n+2| + \text{h.c.})$
- $t_{e/2}$ represents tunneling of a domain wall between two degenerate magnetic states



Hamiltonian in the degenerate ground state

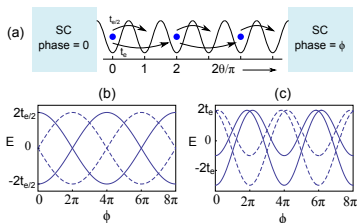


(a) Strong interactions pin the charge between the superconductors and lead to a fourfold ground state degeneracy. Charge $e/2$ or charge e tunneling processes lift the degeneracy, with an 8π periodicity in ϕ , as shown in (b) for $t_e = 0$ and (c) for $t_e = 2t_{e/2}$. Solid and dashed lines correspond to states with opposite fermion parity.

- $|n\rangle$ denotes the state $\theta = n\pi/2$, (with n defined modulo 4)
- $H = \sum_{n=1}^4 (-t_{e/2} e^{i\frac{\phi}{4}} |n\rangle\langle n+1| - t_e e^{i\frac{\phi}{2}} |n\rangle\langle n+2| + \text{h.c.})$
- $t_{e/2}$ represents tunneling of a domain wall between two degenerate magnetic states
- $E_{m=1,2,3,4} = -2t_{e/2} \cos[(\phi - 2\pi m)/4] - 2t_e \cos[(\phi - 2\pi m)/2]$



Hamiltonian in the degenerate ground state

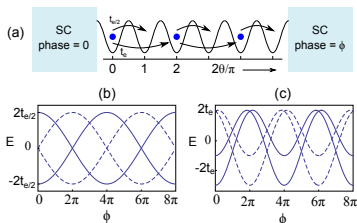


(a) Strong interactions pin the charge between the superconductors and lead to a fourfold ground state degeneracy. Charge $e/2$ or charge e tunneling processes lift the degeneracy, with an 8π periodicity in ϕ , as shown in (b) for $t_e = 0$ and (c) for $t_e = 2t_{e/2}$. Solid and dashed lines correspond to states with opposite fermion parity.

- $|n\rangle$ denotes the state $\theta = n\pi/2$, (with n defined modulo 4)
- $H = \sum_{n=1}^4 (-t_{e/2} e^{i\frac{\phi}{4}} |n\rangle\langle n+1| - t_e e^{i\frac{\phi}{2}} |n\rangle\langle n+2| + \text{h.c.})$
- $t_{e/2}$ represents tunneling of a domain wall between two degenerate magnetic states
- $E_{m=1,2,3,4} = -2t_{e/2} \cos[(\phi - 2\pi m)/4] - 2t_e \cos[(\phi - 2\pi m)/2]$
- Guarantees an 8π periodicity when ϕ is advanced adiabatically



Hamiltonian in the degenerate ground state



(a) Strong interactions pin the charge between the superconductors and lead to a fourfold ground state degeneracy. Charge $e/2$ or charge e tunneling processes lift the degeneracy, with an 8π periodicity in ϕ , as shown in (b) for $t_e = 0$ and (c) for $t_e = 2t_{e/2}$. Solid and dashed lines correspond to states with opposite fermion parity.

- $|n\rangle$ denotes the state $\theta = n\pi/2$, (with n defined modulo 4)
- $H = \sum_{n=1}^4 (-t_{e/2} e^{i\frac{\phi}{4}} |n\rangle\langle n+1| - t_e e^{i\frac{\phi}{2}} |n\rangle\langle n+2| + \text{h.c.})$
- $t_{e/2}$ represents tunneling of a domain wall between two degenerate magnetic states
- $E_{m=1,2,3,4} = -2t_{e/2} \cos[(\phi - 2\pi m)/4] - 2t_e \cos[(\phi - 2\pi m)/2]$
- Guarantees an 8π periodicity when ϕ is advanced adiabatically
- **Thank you:** Comments + Questions ???